Inorganic Chemistry

Article

pubs.acs.org/IC

Synthesis, Properties, and Complex Crystal Structure of Th_2Se_5

Brian J. Bellott, Christos D. Malliakas, Lukasz A. Koscielski, Mercouri G. Kanatzidis, and James A. Ibers*

Department of Chemistry, Northwestern University, 2145 Sheridan Road, Evanston, Illinois 60208-3113, United States

Supporting Information

ABSTRACT: The compound Th_2Se_5 has been synthesized and its structure determined by means of single-crystal X-ray diffraction methods. The subcell of Th_2Se_5 is in the tetragonal space group $P4_2/nmc$ and is isostructural to Np_2Se_5. The modulated structure of Th_2Se_5 has been solved in the monoclinic super space group $P2(\alpha 0\gamma)0$. The structure features parallel infinite Se−Se chains with minimum and maximum Se−Se distances of 2.477(5) and 2.967(5) Å, respectively. Th_2Se_5 is a semiconductor with an electrical resistivity that shows thermally activated Arrhenius behavior with an activation energy of 0.40(1) eV. From spectroscopic measurements, the band gap of Th_2Se_5 is 0.37(2) eV. That the Th_2Se_5 structure is modulated whereas the Np_2Se_5 structure appears not to be implies that the formal oxidation state of Np in Np_2Se_5 is 4+.

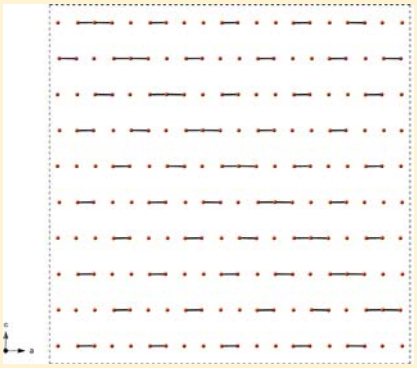

INTRODUCTION

Actinide chalcogenides, An_xQ_y (An = Th, U, or Np; Q = S or Se) display unique chemical and physical properties owing to their accessible and partially filled 5f orbitals.[1,2] Actinide binary materials display a range of formal oxidation states, electronic properties, magnetic properties, and crystal structures.[3,4] Five An_2Q_5 compounds have been reported (U_2S_5,[5] Th_2S_5,[5−8] Th_2Se_5,[5,6,8] Np_2S_5,[9−12] and Np_2Se_5[11−15]). The structure of Th_2S_5 has been refined from single-crystal X-ray diffraction data and is reported to have orthorhombic pseudotetragonal symmetry.[7] The symmetries of the other four An_2Q_5 compounds have been determined from analyses of X-ray powder diffraction data and are in agreement with that of Th_2S_5.[8] Examination of the Th_2S_5 X-ray powder diffraction pattern revealed that the difference between the lengths of the *a* and *b* axes [0.054(8) Å] was sufficient to resolve reflection splitting indicative of symmetry lower than tetragonal.[7] For Th_2Se_5, the difference between the lengths of *a* and *b* was 0.016(1) Å, which was not sufficient to resolve reflection splitting, but line broadening between 0.14° and 0.20° was observed.[8]

Here, we report the synthesis of Th_2Se_5 from the combination of Th and Se in an Sb_2Se_3 flux. Single-crystal X-ray diffraction measurements show that the structure of Th_2Se_5 is modulated. We show that the unmodulated structure (the "subcell") is tetragonal and isostructural to Np_2Se_5; we then present the modulated structure, which is of monoclinic symmetry. The subcell structure features parallel infinite Se−Se chains with distances of 2.721(2) and 2.880(2) Å. Our refinement of the incommensurate structure shows that these are phantom distances and that, in the modulated structure, which is driven by the need to form normal Se−Se bonds, the minimum and maximum Se−Se bonds are 2.447(5) and 2.967(5) Å, respectively, in length.

EXPERIMENTAL METHODS

Syntheses. Th (MP Biomedicals), Se (Cerac, 99.999%), and Sb (Aldrich, 99.5%) were used as received. Sb_2Se_3 was prepared from the direct reaction of the elements in a sealed fused-silica tube at 1123 K.

Reactants were loaded into a carbon-coated fused-silica tube in an Ar-filled glovebox. The tube was loaded with Th (24 mg, 0.103 mmol), Se (21 mg, 0.266 mmol), and Sb_2Se_3 (100 mg, 0.208 mmol). The tube was evacuated to near 10^{-4} Torr; flame-sealed; placed in a computer-controlled furnace; and heated to 1173 K in 24 h, then to 1223 K in 24 h, kept at 1223 K for 48 h, cooled to 1173 K in 24 h, then cooled to 673 K in 150 h, and finally cooled to 298 K in 24 h. Crystals of Th_2Se_5 were obtained in nearly 100 wt % yield based on Th, with the remaining product being metallic black rods of crystallized Sb_2Se_3. The elemental composition of the crystals, determined on an energy-dispersive-X-ray- (EDX-) equipped Hitachi S-3400 scanning electron microscope, contained only Th and Se in the approximate ratio of 2:5. The compound Th_2Se_5 appears to be thermodynamically stable, as it can be found as a side product in many reactions containing Th and Se.

Structure Determinations. Single-crystal X-ray diffraction data for Th_2Se_5 were collected with the use of graphite-monochromatized Cu Kα radiation (λ = 1.54178 Å) at 100 K on a Bruker APEX2 diffractometer.[16] The data collection strategy was optimized with the algorithm COSMO in the program APEX2[16] as a series of 0.3° scans in φ. The exposure time was 5 s/frame. The crystal-to-detector distance was 6 cm. The collection of intensity data, cell refinement, and data reduction were carried out with the use of the program APEX2.[16] Face-indexed-absorption, incident-beam, and decay corrections were performed with the use of the program SADABS.[17] The subcell was solved and refined with the program suite SHELXTL.[18] The atomic positions were standardized with the program STRUCTURE TIDY.[19] Molecular graphics were generated with the software CrystalMaker.[20]

Tetragonal Subcell. The subcell structure of Th_2Se_5 is in space group $P4_2/nmc$ of the tetragonal system. Two formula units are

Received: October 3, 2012
Published: December 27, 2012

 © 2012 American Chemical Society

present in a cell of dimensions a = 5.6012 (1) Å, c = 10.6897(3) Å. Of the total of 6454 reflections, 3785 were rejected, 43 were systematic absence violations, and 153 unique reflections resulted. Additional details are presented in Table 1 and in the Supporting Information.

Table 1. Crystal Data and Structure Refinement for the Subcell of Th_2Se_5[a]

color	copper
space group	$P4_2/nmc$
Fw	858.88
Z	2
a (Å)	5.6010(1)
c (Å)	10.6897(3)
V (Å^3)	335.373(9)
ρ_c (g cm^{-3})	8.505
μ (mm^{-1})	172.05
$R(F)$[b]	0.0233
$R_w(F^2)$[c]	0.0986

[a] λ = 1.54178 Å, T = 100(2) K. [b] $R(F) = \sum||F_o| - |F_c||/\sum|F_o|$ for $F_o^2 > 2\sigma(F_o^2)$. [c] $R_w(F_o^2) = \{\sum[w(F_o^2 - F_c^2)^2]/\sum wF_o^4\}^{1/2}$ for all data. $w^{-1} = \sigma^2(F_o^2) + (0.0381F_o^2)^2$ for $F_o^2 \geq 0$; $w^{-1} = \sigma^2(F_o^2)$ for $F_o^2 < 0$.

The large number of rejected reflections arises from ignoring a larger tetragonal cell (see Figure 1) in which a length is $a_{subcell} \times 2^{1/2}$. Integration of that cell leads to a "tetragonal supercell" (see Appendix A in the Supporting Information).

Modulated Structure. As can be seen in Figure 1, which is a "precession" picture derived within APEX2 from the diffraction frames, the single-crystal X-ray diffraction data show clear indications that the structure is modulated. Atomic coordinates of the atoms in the subcell and initial values of their modulation functions were determined by the charge-flipping method.[21,22] The structure was refined with JANA2006 software.[23] The refinement of the q vectors was performed with the NADA software[23] using a least-squares refinement algorithm. In total, 1802 satellite reflections of first order, with 1408 above the $I > 2\sigma(I)$ limit, were observed at 100 K and used for the refinement. One modulation wave for the positional parameters was used for all atoms. One modulation wave for the displacement parameters was used for all Th atoms because no further improvement of the refinement was achieved when the corresponding displacement parameters for the Se atoms were introduced. Only the symmetry-allowed Fourier terms were refined.

The refinement program used the periodic modulation function $p(x_4) = p(x_4 + n)$, where n is an integer number to describe the changes of the basic structural parameters along the modulation vector. Owing to the periodicity, the distortion (positional, occupational, displacement parameter) of a given atomic parameter x_4 of the subcell can be expressed by a periodic modulation function $p(x_4)$ in the form of a Fourier expansion

$$p(k + x_4) = \sum_{n=1}^{m} A_{sn} \sin[2\pi\cdot\bar{\mathbf{q}}_n(k + x_4)] + \sum_{n=1}^{m} A_{cn} \cos[2\pi\cdot\bar{\mathbf{q}}_n(k + x_4)] \quad (1)$$

where A_{sn} is the sinusoidal coefficient of the given Fourier term, A_{cn} is the cosine coefficient, n is the number of modulation waves used for the refinement, k is the lattice translation, and $\bar{\mathbf{q}}_n = \sum_{i=1}^{d}\alpha_{ni}\mathbf{q}_i$, where α_{ni} represents integers for the linear combination of the incommensurate modulation vectors $\mathbf{q}_i$. The number of terms used depends on the complexity of the modulation function and, therefore, on the order of the observed satellites. The coordinate t that characterizes and describes the real three-dimensional structure constructed as a perpendicular intersection with the fourth-dimensional axis is defined as $t = x_4 - \mathbf{q}\cdot\mathbf{r}$, where $\mathbf{r}$ is a vector in the real three-dimensional reciprocal space. Additional details are presented in Table 2 and in the Supporting Information.

Electrical Resistivity Measurements. Four-probe high-temperature electrical resistivity measurements were performed from 293 to 500 K on the crystal used for the X-ray data collection. Measurements were made for arbitrary current directions in the *ac* pseudotetragonal plane using standard four-point contact geometry. A homemade resistivity apparatus equipped with a Keithley 2182A nanovoltmeter, a Keithley 6220 Precision direct-current (dc) source, and a high-temperature vacuum chamber controlled by a K-20 MMR system was used. Data acquisition was controlled by custom-written software.

Band Gap Measurements. A Nicolet 6700 IR spectrometer equipped with a diffuse-reflectance kit was used for the 4000−400 cm^{-1} spectral region. The spectrum was referenced against a metallic mirror used as a nonabsorbing reflectance standard. The generated reflectance-versus-wavelength data were used to estimate the band gap of the material by converting reflectance to absorbance data according to the Kubelka−Munk equation: $\alpha/S = (1 - R)^2/(2R)$, where R is the reflectance and α and S are the absorption and scattering coefficients, respectively.[24−26]

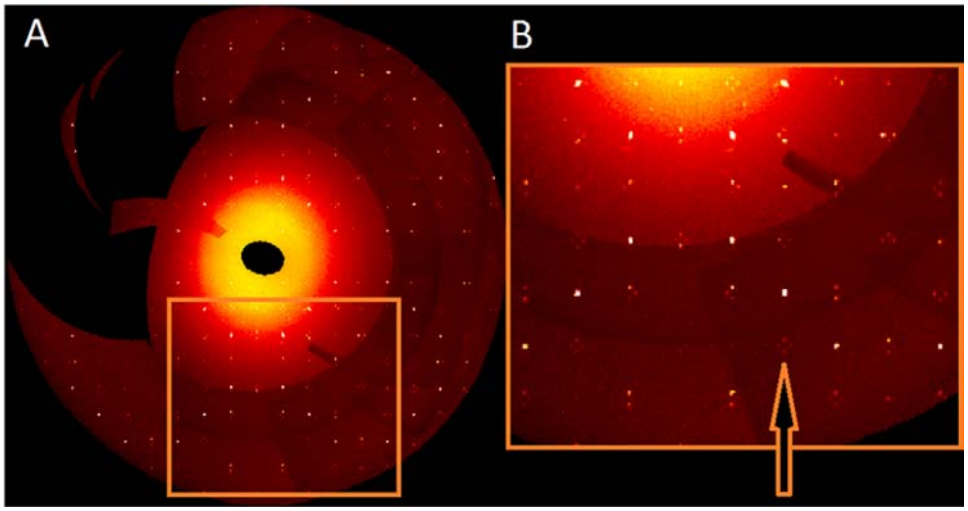

Figure 1. (A) An *hk*1 precession pattern simulated in APEX2 from a crystal of Th_2Se_5. (B) Magnification of selection outlined in panel A. The arrow points to satellite reflections caused by modulation.

dx.doi.org/10.1021/ic302154p | *Inorg. Chem.* 2013, 52, 944−949

Table 2. Crystal Data and Structure Refinement for the Modulated Structure of Th_2Se_5

empirical formula	Th_2Se_5
formula weight	858.9
temperature	100.0(3) K
wavelength	1.54178 Å
crystal system	monoclinic
space group	$P2(\alpha 0\gamma)0$
unit cell dimensions	a = 5.6030(4) Å
	b = 10.6920(6) Å, β = 90°
	c = 5.6030(4) Å
q vector(1)	$0.4464(5)a^* + 0.4464(5)c^*$
volume	335.66(4) Å^3
Z	2
density (calculated)	8.495 g/cm^3
absorption coefficient	171.9 mm^{-1}
F(000)	700
crystal size	0.071 mm × 0.040 mm × 0.009 mm
θ range for data collection	6.19 to 66.98°
index ranges	$-7 \le h \le 6, -12 \le k \le 10, -7 \le l \le 6, -1 \le m \le 1$
reflections collected	11846 (3741 main + 8105 satellites)
independent reflections	2709 (875 main + 1834 satellites) [R_{int} = 0.0266]
completeness to θ = 66.98°	98%
refinement method	full-matrix least-squares on F^2
data/constraints/restraints/parameters	2709/1/0/114
goodness of fit on F^2	1.27
final R indices[a] [$I > 2\sigma(I)$]	R_{obs} = 0.0349, wR_{obs} = 0.1334
R indices[a] (all data)	R_{all} = 0.0394, wR_{all} = 0.1370
final R main indices[a] [$I > 2\sigma(I)$]	R_{obs} = 0.0306, wR_{obs} = 0.1467
R main indices[a] (all data)	R_{all} = 0.0313, wR_{all} = 0.1480
final R first-order satellites[a] [$I > 2\sigma(I)$]	R_{obs} = 0.0501, wR_{obs} = 0.1192
R first-order satellites[a] (all data)	R_{all} = 0.0669, wR_{all} = 0.1255
extinction coefficient (×10^{-1})	164(9)
T_{min} and T_{max} coefficients	0.0071 and 0.2645
largest difference, peak and hole	1.92 and −1.82 e$^-$ Å^{-3}

[a] $R(F) = \sum||F_o| - |F_c||/\sum|F_o|$ for $F_o^2 > 2\sigma(F_o^2)$. $wR = \{\sum[w(F_o^2 - F_c^2)^2]/\sum[w(F_o^4)]\}^{1/2}$ and $w = 1/[\sigma^2(I) + 0.0064I^2]$.

RESULTS

Synthesis. Single crystals of Th_2Se_5 were synthesized in 100 wt % yield by the stoichiometric reaction in an Sb_2Se_3 flux of Th and Se at 1223 K.

Structure of the Subcell. The Th_2Se_5 substructure is the same as the structure of Np_2Se_5.[15] It comprises two formula units in the tetragonal space group $P4_2/nmc$. There are one crystallographically independent Th atom and two crystallographically independent Se atoms. The site symmetries of Th1, Se1, and Se2 are 2*mm*., .*m*., and $\bar{4}m2$, respectively. Table 3 presents some comparative metrical data for the Th_2Se_5 substructure and the structure of Np_2Se_5.

The structure is a complex network comprising infinite linear chains of Se atoms running along the *a* and *b* axes (Figure 2). Atom Th1 is coordinated by a polyhedron of 10 Se atoms. However, if one considers the centers of the Se−Se pairs, then the coordination can be described as octahedral. Each Se atom is coordinated by four Th atoms. The Th−Se distances in Th_2Se_5 range from 3.0095(2) to 3.1464(5) Å, whereas in $ThSe_2$ the range is from 2.8598(1) to 3.2882(1) Å.[27] In ThSe, the Th−Se distance is 2.9448(1)Å.[28] The Se1−Se1−Se1 infinite chains have alternating distances of 2.721(2) and 2.880(2) Å. These distances, although comparable to those in $CsTh_2Se_6$,[29] are phantom because the true structure is actually modulated.

Table 3. Interatomic Distances (Å) for the Th_2Se_5 Subcell and for Np_2Se_5

distance	Th_2Se_5	Np_2Se_5
An1−Se2 × 2	3.0095(2)	2.9284(2)
An1−Se1 × 2	3.0219(9)	2.9861(4)
An1−Se1 × 2	3.0497(9)	3.0270(4)
An1−Se1 × 4	3.1464(5)	3.0686(3)
Se1−Se1	2.721(2)	2.6489(8)
Se1−Se1	2.880(2)	2.7999(8)

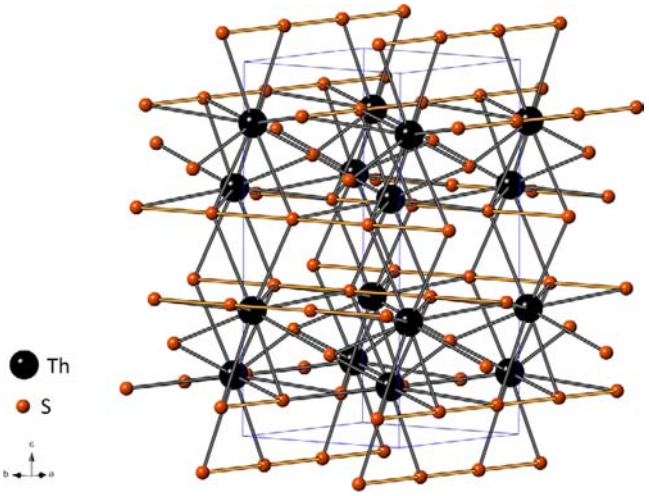

Figure 2. Subcell structure of Th_2Se_5. The unit cell is outlined.

Modulated Structure. A Rietveld refinement[8] of X-ray powder diffraction data for Th_2S_5 in the orthorhombic space group $Pcnb$[7] was satisfactory. The orthorhombic symmetry of Th_2S_5 was not in doubt because some doubling of X-ray powder diffraction powder lines had been observed earlier.[7] A similar Rietveld refinement[8] of X-ray powder diffraction data for Th_2Se_5 based on the structural model of Th_2S_5 was also deemed satisfactory, although no splitting of the reflections was observed and the cell and reflection conditions were equally compatible with the tetragonal space group $P4_2/nmc$. Nevertheless it was suggested that the An_2Q_5 compounds (An = Th, U, Np; Q = S, Se) are all orthorhombic, albeit pseudotetragonal.[8] However, in the single-crystal X-ray diffraction data of Th_2Se_5 described here, there is no evidence of overlapping spots. In particular, intense high-angle subcell *hk*0 reflections on the frames showed no splitting or broadening.

Figure 1 shows that, upon close inspection, reflections that result from modulation are evident. These extra reflections appear as groups of four closely spaced weak reflections between more intense singular spots. Accordingly, the single-crystal X-ray diffraction data were integrated and refined with the reported pseudotetragonal subcell $a = c = 5.6030(4)$ Å, $b = 10.6920(6)$ Å, and a diagonal incommensurate modulation vector of $q = 0.4464(5)a^* + 0.4464(5)c^*$. The monoclinic crystal system was found to be the only high-symmetry option consistent with the orientation and symmetry of the modulation vector. According to the extinction analysis of the collected reflections, the superspace group selection was limited

dx.doi.org/10.1021/ic302154p | Inorg. Chem. 2013, 52, 944−949

to $P2_1(\alpha 0\gamma)0$, $P2_1/m(\alpha 0\gamma)00$, $P2/m(\alpha 0\gamma)00$, $Pm(\alpha 0\gamma)0$, and $P2(\alpha 0\gamma)0$. Stable refinement was achieved in the monoclinic superspace group $P2(\alpha 0\gamma)0$, with the rest of the monoclinic options having overall agreement factors greater than 30%. In total, 10 atomic positions in the asymmetric unit cell were used. The overall agreement factor refined to 0.0349 for all observed $[I > 2\sigma(I)]$ reflections; the agreement factors for the subcell reflections and the first-order satellite reflections were 0.0306 and 0.0501, respectively. Owing to the pseudotetragonal symmetry of the subcell, a 90° rotation along the b axis, namely, twin law $[0\ 0\ 1\ 0\ 1\ 0\ -1\ 0\ 0]$, was included with a refined fraction of 28.7(6)%.

The distortions arising from the modulation are mainly located in the linear Se−Se−Se chains, where a wide distribution of Se−Se distances is observed. The shortest distance between Se atoms in a chain is 2.447(5) Å, and the maximum interatomic distance is 2.967(5) Å. These values are significantly different from the average undistorted Se−Se separation of 2.745(5) Å. The fractions of Se−Se distances below 2.6, 2.7, and 2.8 Å are around 52%, 55%, and 59%, respectively. A representative view of the Se oligomers in the incommensurate cell is shown in Figure 3. The coordination

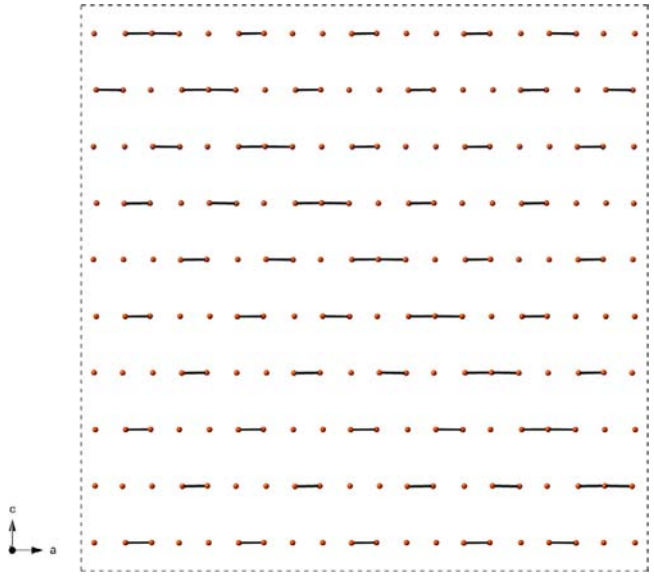

Figure 3. Pattern of Se oligomers in the incommensurately modulated structure. The Se−Se bonding threshold is 2.70 Å. A 10 a × 10 c-fold section of the subunit cell is shown.

geometry about the Th atoms is also affected by the distortions. The shortest interatomic Th−Se distance is 2.980(4) Å, and the maximum distance is 3.242(3) Å. The corresponding plots of Se−Se and Th−Se distances along the modulation direction are shown in Figures 4 and 5, respectively.

Electrical Resistivity. High-temperature resistivity measurement on a single crystal of Th_2Se_5 showed semiconducting behavior. The resistivity at 293 K decreases from 225 to 0.42 Ω cm at 500 K. A logarithmic plot of the resistivity as a function of temperature is shown in Figure 6A. The corresponding Arrhenius plot is linear for the whole temperature range, indicative of a simple mechanism of carrier excitation with an activation energy of 0.40(1) eV (Figure 6B).

Band Gap. Optical absorption spectroscopic results at 293 K imply the presence of an energy gap of ~0.37(2) eV (Figure 7). The sharp peak before the absorption edge may be assigned

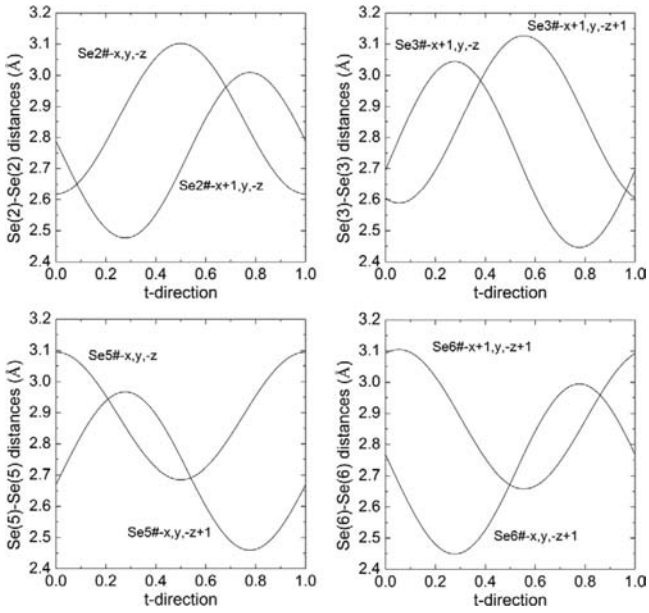

Figure 4. Se−Se distances along the modulation direction within the chains of Se atoms. Symmetry transformations of the generated equivalent atoms are shown next to each curve.

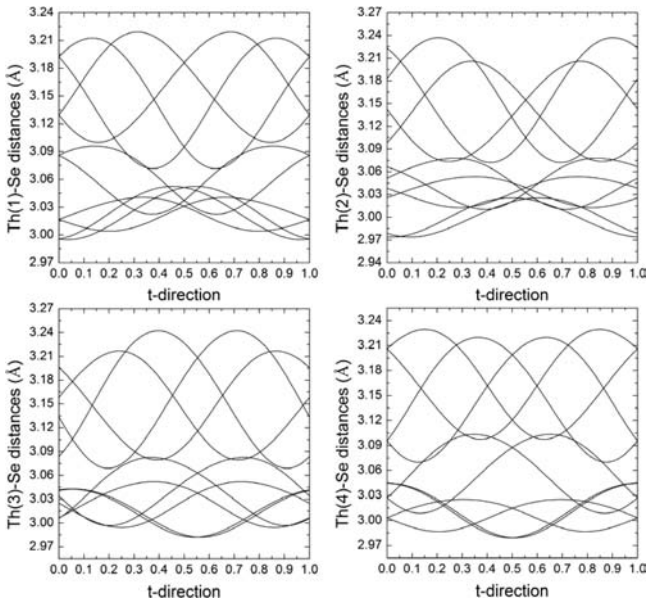

Figure 5. Th−Se distances along the modulation direction. Plots for all four crystallographically independent Th atoms are shown.

to an electronic transition between Se p states and Th f states, in accord with simple ionic models with the Th^{4+} $6p^6 6d^0 7s^0 5f^0$ configuration.[30]

DISCUSSION

Whereas single-crystal X-ray diffraction data for Th_2Se_5 show modulation (Figure 1), those for Np_2Se_5[15] do not. There are several possible explanations for the difference in these structures. One possibility, which seems improbable, is in the choice of crystals. Perhaps other crystals of Th_2Se_5 would display only the subcell or another crystal of Np_2Se_5 would show modulation.

A comparison of the interatomic distances in the subcell (Table 3) indicates that the average decrease in An−Se

dx.doi.org/10.1021/ic302154p | Inorg. Chem. 2013, 52, 944−949

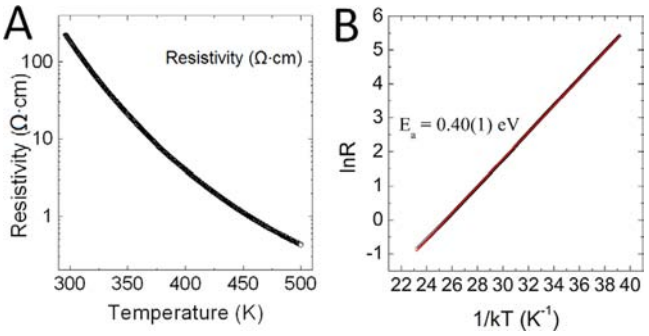

Figure 6. (A) Temperature-dependent resistivity of a Th_2Se_5 single crystal showing semiconducting behavior. (B) Arrhenius plot (black circles) and linear fit (red line) of the resistivity data. An activation energy of 0.40(1) eV was calculated.

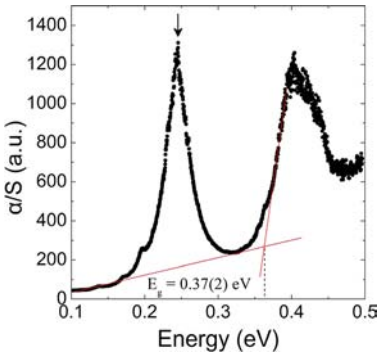

Figure 7. Absorption spectrum of Th_2Se_5 at 293 K showing a band gap of 0.37(2) eV. The peak marked with an arrow before the absorption edge can be assigned to an electronic transition between Se p states and Th f states.

distances in going from An = Th to An = Np is 0.059 Å. This is consistent with the decrease of 0.07 Å in crystal radii[31] as one goes from six-coordinate Th^{4+} (0.94 Å) to six-coordinate Np^{4+} (0.87 Å). These "phantom" Th−Se distances in Table 3 change little in the modulated structure, where the average Th−Se distances range from 3.000 to 3.166 Å. If one assumes that the crystals chosen for both substances are typical, then steric hindrance, including that arising from distortions in the infinite Se−Se chains[32,33] and that arising from the increased size of Th^{4+} compared to Np^{4+}, is the most likely cause of an incommensurate structure, particularly when the structure has a framework of connected polyhedra.[34] The formal oxidation state of Th is 4+ in known chalcogenides, whereas there are well-documented examples of Np in both the 3+ and 4+ formal oxidation states. Note that the crystal radius of six-coordinate Np^{3+} is 1.01 Å. That Th^{4+} is large enough to bring about steric hindrance and hence modulations implies that Np^{3+}, being larger, should also. Thus, the fact that the Th_2Se_5 structure is modulated whereas the Np_2Se_5 is not strongly suggests that the formal oxidation state of Np in Np_2Se_5 is 4+.

CONCLUSIONS

Single crystals of the compound Th_2Se_5 have been synthesized by the reaction in an Sb_2Se_3 flux of Th and Se at 1223 K. The structure of Th_2Se_5 was determined by means of single-crystal X-ray diffraction methods. The subcell of Th_2Se_5 is in the tetragonal space group $P4_2/nmc$ with a = 5.6012(1) Å and c = 10.6897(3) Å. It is isostructural with Np_2Se_5. However, the structure of Th_2Se_5 is modulated and has been solved in the monoclinic superspace group $P2(\alpha 0\gamma)0$ in a cell of dimensions $a = c$ = 5.6030(4) Å, b = 10.6920(6) Å, with a diagonal incommensurate modulation vector of q = 0.4464(5)a^* + 0.4464(5)c^*. Th_2Se_5 is a semiconductor with an electrical resistivity that shows thermally activated Arrhenius behavior with an activation energy of 0.40(1) eV. From spectroscopic measurements, the band gap of Th_2Se_5 is 0.37(2) eV. That the Th_2Se_5 structure is modulated whereas the Np_2Se_5 structure appears not to be implies that the formal oxidation state of Np in Np_2Se_5 is 4+.

Similar types of modulation and the formation of oligomers among chalcogen atoms have been observed in compounds containing square nets of tellurium atoms; for example, in rare-earth tritellurides.[35] Extended interactions along two dimensions usually create nonlinear distorted oligomers, but the systems are still metallic. When there are linear chains of chalcogen atoms, for example, in $CuUTe_3$,[36] the one-dimensional distortions usually generate semiconducting behavior. Such modulations in metal chalcogenides can be challenging to solve and sometimes even to identify. Given the increased sensitivity of modern X-ray single-crystal diffractometers and accompanying software, we believe that careful reexamination of metal chalcogenides containing linear chains or planar nets is warranted, as such systems are prone to distortion.

ASSOCIATED CONTENT

Supporting Information

Crystallographic file in cif format for the modulated structure of Th_2Se_5. Appendix A, the subcell and supercell of Th_2Se_5. This material is available free of charge via the Internet at http://pubs.acs.org.

AUTHOR INFORMATION

Corresponding Author

*E-mail: ibers@chem.northwestern.edu.

Notes

The authors declare no competing financial interest.

ACKNOWLEDGMENTS

This research was supported at Northwestern University by the U.S. Department of Energy, Basic Energy Sciences, Chemical Sciences, Biosciences, and Geosciences Division and Division of Materials Sciences and Engineering, Grant ER-15522, and by the National Science Foundation (DMR-1104965, M.G.K.). L.A.K. was also supported by the Nuclear Energy University Programs of the U.S. Department of Energy Office of Nuclear Energy. J.A.I. thanks Sander van Smaalen for helpful correspondence.

REFERENCES

(1) Bugaris, D. E.; Ibers, J. A. *Dalton Trans.* **2010**, *39*, 5949−5964.

(2) Manos, E.; Kanatzidis, M. G.; Ibers, J. A. In *The Chemistry of the Actinide and Transactinide Elements*, 4th ed.; Morss, L. R., Edelstein, N. M., Fuger, J., Eds.; Springer: Dordrecht, The Netherlands, 2010; Vol. 6, pp 4005−4078.

(3) Grenthe, I.; Drozdzynski, J.; Fujino, T.; Buck, E. C.; Albrecht-Schmitt, T. E.; Wolf, S. F. In *The Chemistry of the Actinide and Transactinide Elements*, 3rd ed.; Morss, L. R., Edelstein, N. M., Fuger, J., Eds.; Springer: Dordrecht, The Netherlands, 2006; Vol. *1*, pp 253−698.

(4) Yoshida, Z.; Johnson, S. G.; Kimura, T.; Krsul, J. R. In *The Chemistry of the Actinide and Transactinide Elements*, 3rd ed.; Morss, L.

R., Edelstein, N. M., Fuger, J., Eds.; Springer: Dordrecht, The Netherlands, 2006; Vol. 2, pp 699−812.
(5) Noël, H. *J. Inorg. Nucl. Chem* **1980**, *42*, 1715−1717.
(6) Graham, J.; McTaggart, F. K. *Aust. J. Chem.* **1960**, *13*, 67−73.
(7) Noël, H.; Potel, M. *Acta Crystallogr. B: Struct. Crystallogr. Cryst. Chem.* **1982**, *38*, 2444−2445.
(8) Kohlmann, H.; Beck, H. P. *Z. Kristallogr.* **1999**, *214*, 341−345.
(9) Marcon, J.-P. *C. R. Seances Acad. Sci., Ser. C* **1967**, *265*, 235−237.
(10) Marcon, J.-P. *Commis. Energ. At. [Fr.], Rapp.* **1969**, *CEA-R-3919*, 1−99.
(11) Thévenin, T. Ph.D. Dissertation, Paris 11 University, Orsay, France, 1982.
(12) Spitsyn, V. I.; Ionova, G. V. *Dokl. Akad. Nauk SSR* **1987**, *293*, 920−922.
(13) Thévenin, T.; Jové, J.; Pagès, M. *Mater. Res. Bull.* **1985**, *20*, 723−730.
(14) Thévenin, T.; Pagès, M.; Wojakowski, A. *J. Less-Common Met.* **1982**, *84*, 133−137.
(15) Jin. G. B.; Hu, Y.-J.; Bellott, B. J.; Skanthakumar, S.; Haire, R. G.; Soderholm, S.; Ibers, J. A., in preparation.
(16) *Bruker APEX2 Version 2009.5-1 and SAINT Version 7.34a Data Collection and Processing Software*; Bruker Analytical X-ray Instruments, Inc.: Madison, WI, 2009.
(17) Sheldrick, G. M. *SADABS*; University of Göttingen, Göttingen, Germany, 2008.
(18) Sheldrick, G. M. *Acta Crystallogr. A: Found. Crystallogr.* **2008**, *64*, 112−122.
(19) Gelato, L. M.; Parthé, E. *J. Appl. Crystallogr.* **1987**, *20*, 139−143.
(20) Palmer, D. *CrystalMaker Software*, version 2.2.3; CrystalMaker Software Ltd.: Oxford, U.K., 2009.
(21) Oszlanyi, G.; Suto, A. *Acta Crystallogr. A* **2004**, *60*, 134.
(22) Oszlanyi, G.; Suto, A. *Acta Crystallogr. A* **2005**, *61*, 147.
(23) Petricek, V.; Dusek, M.; Palatinus, L. In *The Crystallographic Computing System*; Institute of Physics: Praha, Czech Republic, 2006.
(24) Kortüm, G. *Reflectance Spectroscopy: Principles, Methods, Applications*; Springer-Verlag: New York, 1969.
(25) Tandon, S. P.; Gupta, J. P. *Phys. Status Solidi B* **1970**, *38*, 363−367.
(26) Wendlandt, W. W.; Hecht, H. G. *Reflectance Spectroscopy*; Interscience: New York, 1966.
(27) D'Eye, R. W. M. *J. Chem. Soc.* **1953**, *75*, 1670−1672.
(28) Olsen, J. S.; Gerward, L.; Benedict, U.; Luo, H.; Vogt, O. *High Temp. - High Pressures* **1988**, *20*, 553−559.
(29) Bugaris, D. E.; Wells, D. M.; Yao, J.; Skanthakumar, S.; Haire, R. G.; Soderholm, L.; Ibers, J. A. *Inorg. Chem.* **2010**, *49*, 8381−8388.
(30) Koscielski, L. A.; Ringe, E.; Van Duyne, R. P.; Ellis, D. E.; Ibers, J. A. *Inorg. Chem.* **2012**, *51*, 8112−8118.
(31) Shannon, R. D. *Acta Crystallogr. A* **1976**, *32*, 751−767.
(32) Choi, K.-S.; Patschke, R.; Billinge, S. J. L.; Waner, M. J.; Dantus, M.; Kanatzidis, M. G. *J. Am. Chem. Soc.* **1998**, *120*, 10706−10714.
(33) Bugaris, D. E.; Wells, D. M.; Yao, J.; Skanthakumar, S.; Haire, R. G.; Soderholm, L.; Ibers, J. A. *Inorg. Chem.* **2010**, *49*, 8381−8388.
(34) Janssen, T.; Chapus, G.; de Boissieu, M. *Aperiodic Crystals*; Oxford University Press: New York, 2007; Chapter 5.
(35) Malliakas, C.; Billinge, S. J. L.; Kim, H. J.; Kanatzidis, M. G. *J. Am. Chem. Soc.* **2005**, *127*, 6510.
(36) Patschke, R.; Breshears, J. D.; Brazis, P.; Kannewurf, C. R.; Billinge, S. J. L.; Kanatzidis, M. G. *J. Am. Chem. Soc.* **2001**, *123*, 4755.